Available online at www.sciencedirect.com
ScienceDirect
Ceramics International 35 (2009) 3221–3227
CERAMICS INTERNATIONAL
www.elsevier.com/locate/ceramint

# Effect of some rare-earth oxides on structure, devitrification and properties of diopside based glasses

Ishu Kansal [a], Ashutosh Goel [a], Dilshat U. Tulyaganov [a,b], José M.F. Ferreira [a,*]

[a] Department of Ceramics and Glass Engineering, University of Aveiro, CICECO, 3810-193 Aveiro, Portugal
[b] State Committee of Geology and Mineral Resources, Centre of remote sensing and GIS technologies, 11-A, Shevchenko str., 100060 Tashkent, Uzbekistan

Received 3 March 2009; received in revised form 8 April 2009; accepted 18 May 2009
Available online 18 June 2009

**Abstract**

Four diopside based glasses containing an equimolar concentration of different rare-earth oxides ($La_2O_3$, $Nd_2O_3$, $Gd_2O_3$ and $Yb_2O_3$) respectively, were obtained by melt-quenching technique. Structural and thermal behaviour of the glasses was investigated by density and molar volume, infrared spectroscopy (FTIR), dilatometry, and scanning electron microscopy (SEM). All the glasses exhibited amorphous phase separation. The crystallization behaviour of the glasses was investigated by using differential thermal analysis (DTA). Sintering, crystallization, microstructure, and properties of the glass-ceramics were investigated under non-isothermal heating conditions in the temperature range of 800–900 °C.



*Keywords:* A. Sintering; D. Glass; D. Glass-ceramics; Rare-earth oxides

## 1. Introduction

Glass-ceramics (GCs) offer the possibility of combining the special properties of conventional sintered ceramics with the distinctive characteristics of glasses. It is, however, possible to develop modern GC materials with features unknown so far either in glasses or ceramics or in other materials such as metals or organic polymers. Furthermore, developing GCs demonstrates the advantage of combining various remarkable properties in one material.

GCs based on pyroxenes attract interest in several advanced fields [1–4] as they offer an excellent opportunity to control their properties, thus leading to the possibility of achieving the desired physical properties and high chemical durability. Diopside (here after briefly designated as Di) belongs to the group of inosilicates and is an important member of clinopyroxene group, with composition $CaMgSi_2O_6$. It forms complete solid solution series with hedenbergite ($CaFeSi_2O_6$) and augite, and partial solid solutions with orthopyroxenes, pigeonite and Ca–Al-bearing monoclinic pyroxene, known as Ca-Tschermak ($CaAl_2SiO_6$).

The present study is an attempt to investigate the influence of different rare-earth oxides ($RE_2O_3$) on the structure and crystallization behaviour of diopside based glasses with general composition $Ca_{0.8}Ba_{0.1}Mg_{0.9}Zn_{0.1}Al_{0.1}RE_{0.1}Si_{1.9}O_6$ (RE corresponds to La, Nd, Gd and Yb, respectively). Since, it has already been shown that substitution of ZnO for MgO improves the sintering behaviour of diopside-Ca-Tschermak GCs [6], therefore, a substitution $0.1MgO \leftrightarrow 0.1ZnO$ was attempted in the present investigation. $B_2O_3$ (1.75 mol%) was introduced in all the investigated glass compositions in order to be consistent with our previous study [5]. Table 1 presents the detailed compositions of all the investigated glasses.

## 2. Experimental procedure

High purity powders of $SiO_2$, $CaCO_3$, $BaCO_3$, $MgCO_3$, $Al_2O_3$, ZnO, $H_3BO_3$, $La_2O_3$, $Nd_2O_3$, $Gd_2O_3$ and $Yb_2O_3$ were used. Homogeneous mixtures of batches (~100 g), obtained by ball milling, were calcined at 900 °C and then melted in $Al_2O_3$-crucibles at 1580 °C for 1 h.

Glasses in bulk form were produced by pouring the melts on preheated bronze moulds followed by annealing at 550 °C for

* Corresponding author. Tel.: +351 234 370242; fax: +351 234 370204.
*E-mail address:* jmf@ua.pt (J.M.F. Ferreira).

0272-8842/$36.00 
doi:10.1016/j.ceramint.2009.05.023

Table 1
Composition of glasses.

| Glass | MgO | CaO | BaO | ZnO | $SiO_2$ | $B_2O_3$ | $Al_2O_3$ | $Ln_2O_3$ |
|---|---|---|---|---|---|---|---|---|
| S–La (wt.%) | 14.80 | 18.31 | 6.26 | 3.32 | 46.58 | 2.00 | 2.08 | 6.65 |
| Ln=La (mol.%) | 22.67 | 20.15 | 2.52 | 2.52 | 47.85 | 1.77 | 1.26 | 1.26 |
| S–Nd (wt.%) | 14.77 | 18.27 | 6.24 | 3.32 | 46.48 | 2.00 | 2.08 | 6.85 |
| Ln=Nd (mol.%) | 22.67 | 20.15 | 2.52 | 2.52 | 47.85 | 1.78 | 1.26 | 1.26 |
| S–Gd (wt.%) | 14.69 | 18.17 | 6.21 | 3.30 | 46.23 | 2.00 | 2.06 | 7.34 |
| Ln=Gd (mol.%) | 22.66 | 20.15 | 2.52 | 2.52 | 47.85 | 1.79 | 1.26 | 1.26 |
| S–Yb (wt.%) | 14.59 | 18.05 | 6.17 | 3.28 | 45.93 | 2.00 | 2.05 | 7.93 |
| Ln=Yb (mol.%) | 22.66 | 20.14 | 2.52 | 2.52 | 47.85 | 1.80 | 1.26 | 1.26 |

1 h. The annealing temperature was decided in accordance with our previous study [5]. The glass-powder compacts were produced from glass frits, which were obtained by quenching of glass melts in cold water. The dry frits were milled in high-speed agate mill resulting in fine glass powders with mean particle sizes of 10–15 μm (Coulter LS 230, Beckman Coulter, Fullerton CA; Fraunhofer optical model). Circular disc shaped pellets with Ø 20 mm and thickness ~3 mm were prepared from glass powders by uniaxial pressing (80 MPa). The pellets were sintered under non-isothermal conditions for 1 h at 800 °C, 850 °C and 900 °C, respectively at a slow heating rate of 2 K $min^{-1}$. The possibility of occurrence of phase separation in the glasses was examined by heating the bulk glasses at 700 °C for 1 h at heating rate of 5 K $min^{-1}$.

Infrared spectra of the glasses were obtained using an Infrared Fourier spectrometer (FTIR, model Mattson Galaxy S-7000, USA). For this purpose samples were crushed to powder form, mixed with KBr in the proportion of 1/150 (by weight) and pressed into a pellet using a hand press.

Dilatometry measurements were done on prismatic samples with a cross section of 4 mm × 5 mm (Bahr Thermo Analyze DIL 801 L, Hüllhorst, Germany; heating rate 5 K $min^{-1}$). The glass transition temperature ($T_g$), onset of crystallization ($T_c$) and peak temperature of crystallization ($T_p$) were obtained from differential thermal analysis of fine powders which was carried out in air (DTA-TG, Setaram Labsys, Setaram Instrumentation, Caluire, France) at heating rate ($\beta$) of 5 K $min^{-1}$.

The linear shrinkage during sintering was calculated from the difference of the diameter between the green and the sintered pellets. Archimedes' method (i.e. immersion in diethyl phthalate) was employed to measure the apparent density of the bulk annealed glasses and sintered GCs. The mean values and the standard deviations presented for linear shrinkage and density have been obtained from (at least) 10 different samples.

The amorphous nature of the glasses and presence of crystalline phases in the GCs were determined by X-ray diffraction (XRD) analysis (Rigaku Geigerflex D/Max, C Series, Tokyo, Japan; $CuK_\alpha$ radiation; $2\theta$ angle range 10–80°; step 0.02°/s). Microstructure observations were done on polished (and etched) glasses and GCs using scanning electron microscopy (SEM, Hitachi SU-70, Tokyo, Japan) under secondary electron mode. The etching was performed by immersion of samples in 2 vol.% HF solution for 5 s (glasses) and 2 min (GCs), respectively.

## 3. Results and discussion

### 3.1. Characterization of glasses

#### 3.1.1. Casting ability, physical appearance and microstructural features

Melting at 1580 °C for 1 h was adequate to obtain highly homogenous molten glasses for all the investigated compositions, which, after casting, resulted in bubble-free, homogenous, transparent glasses. All the glasses except S–Nd were yellow while this particular glass (S–Nd) was purple in colour. In general, the appearance of different colours in $RE^{3+}$-doped glasses is due to splitting of 4f levels and can be explained on the basis of *crystal field theory*. The study pertaining to investigate the local environment of $Nd^{3+}$ and its structural role in the glass network has already been attempted [7]. In this regard it has been documented that presence of neodymium results in clustering effect and affects the optical properties of glasses [8]. The different colour of glass S–Nd in the present case may be due to the following reasons: (i) a change in the oxidation state resulting in a change in number of 4f electrons and thus, leading to a different number of possible electronic transitions for otherwise identical conditions (apart from its well known +3 oxidation state, Nd also exhibits +2 and +4 oxidation states [9]); (ii) a change in coordination number, thus resulting in a difference in splitting energy. Previously, Corradi et al. [10] studied the local environment of neodymium in $Na_2O$–$SiO_2$–$Nd_2O_3$ glass system through molecular dynamic simulations and concluded that $Nd^{3+}$ exists preferentially in octahedral coordination in alkali silicate glasses while Loiseau et al. [11], with the help of spectroscopic techniques, showed that Nd occupies a highly distorted 8–9-fold coordinated site in the glass system $SiO_2$–$Al_2O_3$–CaO–$ZrO_2$–$TiO_2$. Therefore, from the physical appearance of glasses, it can be judged that the structure of glass S–Nd differs from the rest of the three investigated glasses. The SEM images of all bulk glasses (heated at 700 °C for 1 h) (Fig. 1) evidenced spinodal decomposition phase separation [12]. The change in type of $RE^{3+}$ had no significant effect on the phase separation in the investigated glasses.

#### 3.1.2. Density and molar volume

The density of the glasses varied between 3.06 and 3.11 g $cm^{-3}$ (Table 2) and increased with an increase in the molecular weight of the RE-oxide present in the glass.

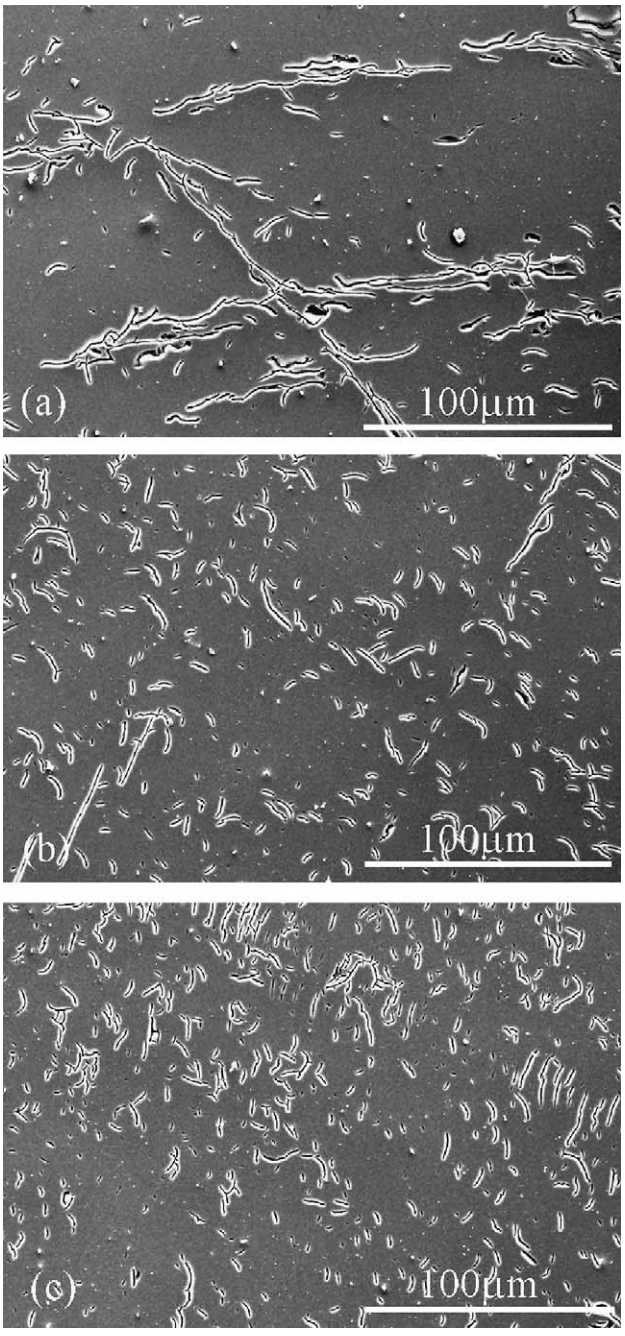


Fig. 1. SEM image of glasses: (a) S–La; (b) S–Nd; and (c) S–Gd, respectively, after heat treatment at 700 °C for 1 h.

The molar volume ($V_m$) was calculated using the apparent density data for the bulk glasses using following relations:

$$V_m = \frac{M}{\rho} \quad (1)$$

where $M$ is the molar mass of the glass and $\rho$ is the apparent density of the bulk glasses. Table 2 presents the values of $V_m$ for all the investigated glasses. Unlike density of glasses, no particular trend could be observed for the $V_m$. The lowest value of $V_m$ was calculated for glass S–Gd while the highest was reported for S–Nd. These results contradict the results of Quintas et al. [13], according to whom, the type of $RE^{3+}$ has no significant effect on the mean compactness of oxygen network of the aluminoborosilicate glass. As expected, $V_m$ should have decreased with decreasing ionic radii (increasing field strength) of $RE^{3+}$, as has been observed where S–La > S–Gd > S–Yb. However, the deviation from the trend for glass S–Nd in conjunction with its different colour from other three glasses points towards the change in the structure of this glass. Therefore, FTIR was employed in order to have a better understanding about the structure of these glasses.

### 3.1.3. FTIR

The room temperature FTIR transmittance spectra of all the four investigated glasses are shown in Fig. 2. All spectra exhibit four broad transmittance bands in the region of 300–1500 $cm^{-1}$. This lack of sharp features is indicative of the general disorder in the silicate network mainly due to a wide distribution of $Q_n$ (polymerization in the glass structure, where $n$ denotes the number of bridging oxygens) units occurring in these glasses. The most intense bands in the 800–1300 $cm^{-1}$ region correspond to the stretching vibrations of the $SiO_4$ tetrahedron with a different number of bridging oxygen atoms while bands in the 300–600 $cm^{-1}$ region are due to bending vibrations of Si–O–Si and Si–O–Al linkages [14,15]. The least intensive bands in the region 650–800 $cm^{-1}$ are related to the stretching vibrations of the Al–O bonds with $Al^{3+}$ ions in 4-fold coordination [15]. The transmittance band in the region 1350–1500 $cm^{-1}$ corresponds to B–O vibrations in [$BO_3$] triangle [15]. In the present study, glasses S–La, S–Gd and S–Yb showed similar IR spectra while a slight shift towards higher wave number in the region 800–1300 $cm^{-1}$ was observed for glass S–Nd thus, signifying towards stronger polymerization in the silicate network. This supports the higher molar volume of

Table 2
Properties of glasses.

| | S–La | S–Nd | S–Gd | S–Yb |
|---|---|---|---|---|
| Density (g $cm^{-3}$) | 3.06 ± 0.004 | 3.06 ± 0.001 | 3.09 ± 0.002 | 3.11 ± 0.002 |
| $V_m$ ($cm^3$ $mol^{-1}$) | 20.18 ± 0.025 | 20.25 ± 0.024 | 20.13 ± 0.025 | 20.18 ± 0.025 |
| CTE ($\times 10^{-6}$) ($K^{-1}$) | 7.78 | 7.55 | 7.59 | 7.18 |
| $T_{g1}$ (°C) | 845 | 857 | 857 | 857 |
| $T_{g2}$ (°C) | 861 | 874 | 873 | 873 |
| $T_c$ (°C) | 884 | 891 | 891 | 891 |
| $T_p$ (°C) | 918 | 920 | 930 | 926 |

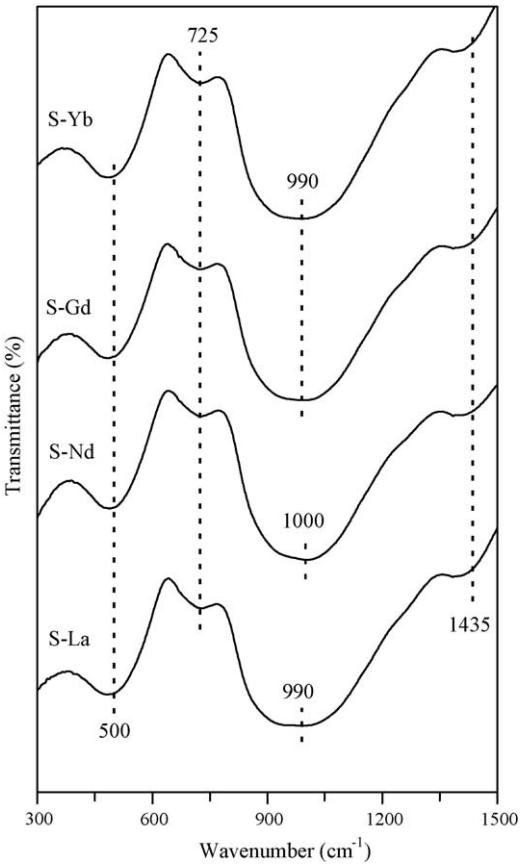


Fig. 2. FTIR spectra of the investigated glass powders.

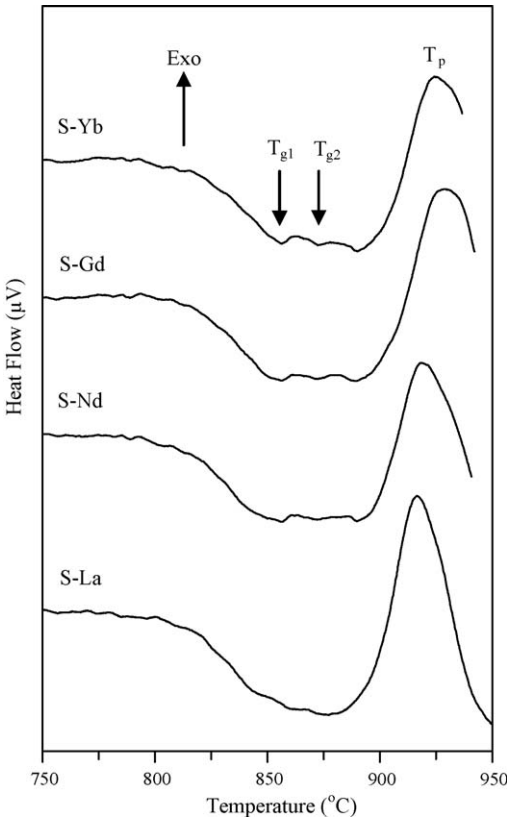


Fig. 3. Differential thermal analysis (DTA) of fine glass powders at heating rate 5 K min$^{-1}$.

the glass S–Nd. In general, results indicate a distribution of $Q_n$ units centred on $Q_2$ and $Q_3$ in all the investigated glasses.

### 3.1.4. Thermal analysis

The values of coefficient of thermal expansion (CTE) for all the four glasses as obtained from linear slope of their thermal expansion curves are presented in Table 2. The highest CTE value was obtained for glass S–La while the lowest was obtained for glass S–Yb. The CTE values in general had a tendency to decrease with increasing field strength of RE-oxides. These results are in accordance with the results reported by Shelby and Kohli [16], where they investigated the CTE of the glasses with composition $20RE_2O_3$–$20Al_2O_3$–$60SiO_2$.

The DTA plots of fine powders with a heating rate of 5 K min$^{-1}$, shown in Fig. 3, featured two endothermic dips ($T_{g1}$ and $T_{g2}$) before the onset of crystallization ($T_c$) indicating the existence of two glass transition temperatures, which is followed by a single exothermic crystallization curve. The existence of two $T_g$ values suggests the possible existence of phase separation in the glasses which is strongly supported by the microstructure of the bulk glasses shown in Fig. 1. The existence of phase separation in diopside based glasses has been well documented in literature [5,17] and is probably caused by the segregation of calcium and magnesium ions in quaternary glass systems CaO–MgO–$Al_2O_3$–$SiO_2$ [18]. The $T_g$ values for all the four glasses are presented in Table 2. It was observed that $T_g$ shifts to higher temperature when $La_2O_3$ (glass S–La) is replaced by $Nd_2O_3$ (S–Nd). However, no further variation in $T_g$ was observed for glasses S–Nd, S–Gd and S–Yb. The slight increase in $T_g$ for glass S–Nd in comparison to glass S–La may be explained on the basis of increasing ionic field strength. However, an explanation for the constant values of $T_g$ for glasses S–Nd, S–Gd and S–Yb needs further structural investigations on these glasses.

The existence of a single crystallization exotherm signifies that either the GC formed as a result of crystallization is mono-mineral or different crystalline phases appear from the glass matrix almost simultaneously and the crystallization curve is the resultant of all these crystalline phases. It was observed that changing the type of RE-ion in the glasses did not affect the crystallization process significantly, as $T_c$ increased slightly for glass S–Nd in comparison to glass S–La. However, similar $T_c$ was observed for all the other three investigated glasses (Table 2). Similarly, $T_p$ for glasses S–La and S–Nd were almost equal while a slight increase in $T_p$ was observed for glass S–Gd (Table 2). A detailed investigation on the isothermal and non-isothermal crystallization kinetics of these glasses is required to better understand the crystallization behaviour of these multi-component glasses.

### 3.2. Characterization of glass-ceramics

In the present case, well-sintered dense glass-powder compacts were obtained after heat treatment at 800 °C for

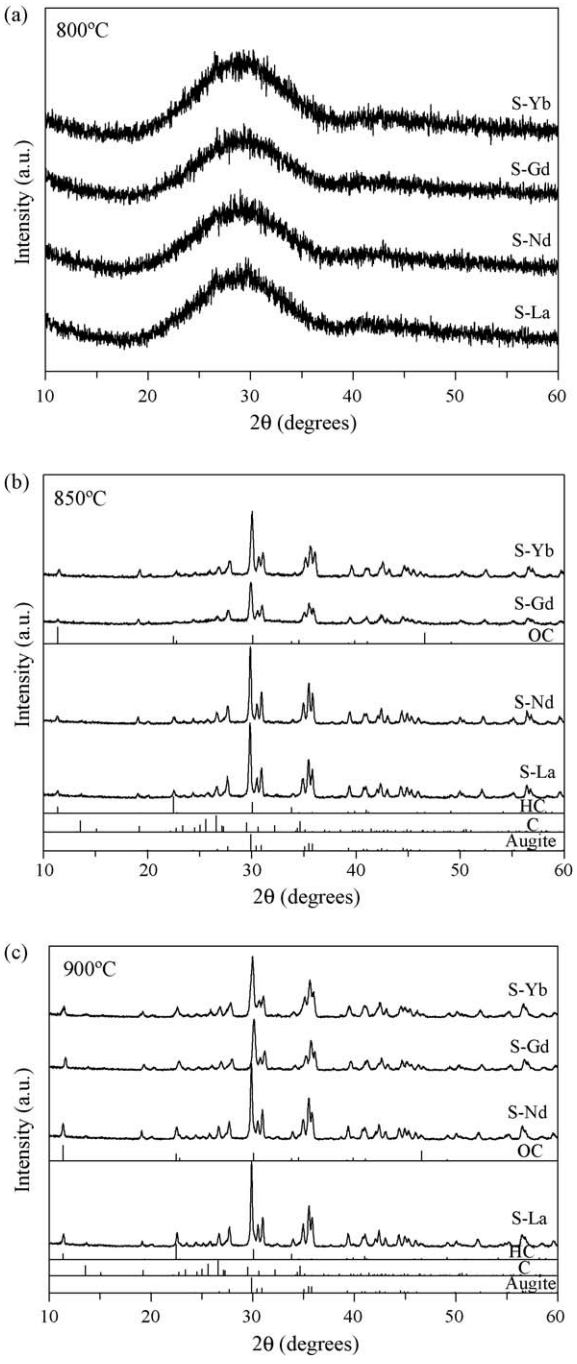


Fig. 4. X-ray diffractograms of glass-powder compacts sintered at (a) 800 °C, (b) 850 °C and (c) 900 °C for 1 h.

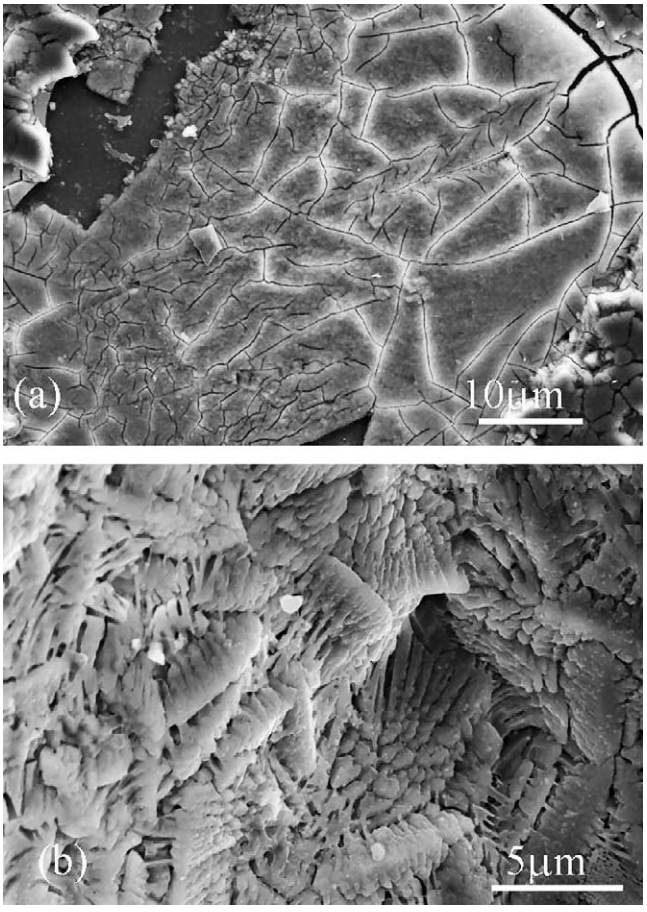


Fig. 5. Microstructure of the GCs S–Gd at: (a) 850 °C; (b) 900 °C.

all the four compositions. Sintering preceded crystallization, as all the compositions were amorphous after heat treatment at 800 °C (Fig. 4a) and the appearance of the samples did not change at higher temperatures. There was no evidence of detrimental effects, such as deformation or formation of open porosity, in the temperature interval of 800–900 °C. Augite ($CaMg_{0.70}Al_{0.30}Si_{1.70}Al_{0.30}O_6$; ICDD card: 01-078-1392) along with different polymorphs of celsian ($BaAl_2Si_2O_8$) i.e. monoclinic celsian (C; $Ba_{0.94}Al_{1.88}Si_{2.12}O_8$; ICDD: 01-071-2536), orthorhombic celsian (OC, ICDD: 00-012-0725) and hexacelsian (HC; ICDD: 01-088-1048) crystallized to be the only crystalline phases in all the GCs heat treated at 850 °C (Fig. 4b) and 900 °C (Fig. 4c). However, the intensity of XRD peaks observed at 850 °C were lower in comparison to those observed at 900 °C, signifying the increase in crystallinity of the GCs with increase in temperature. The XRD results are well supported by the microstructure of the GCs (Fig. 5) where amorphous glassy phase is evident along with crystals (Fig. 5a) after heat treatment at 850 °C while a dense crystalline microstructure was obtained after heat treatment at 900 °C (Fig. 5b). The deviation from the formation of diopside based solid solution and crystallization of celsian may be attributed to the uptake of $Al_2O_3$ from the crucible during melting of the glass as no celsian formation was observed in our previous study on almost similar compositions [4,5].

The density of the GCs increased with an increase in the molecular weight of the RE-oxide, irrespective of the temperature (Fig. 6a). At any particular temperature, the density of the GCs followed the trend S–La<S–Nd < S–Gd < S–Yb. With respect to temperature, the density of all the GCs increased until 850 °C and remained almost constant between 850 °C and 900 °C. The linear shrinkage of all the investigated compositions increased with an increase in temperature and followed the trend S–Nd < S–Gd < S–La < G–Yb (Fig. 6b). Therefore, composition S–Yb showed better sintering ability than all the other three compositions. The CTE of the GCs, except S–Gd, increased with increase in

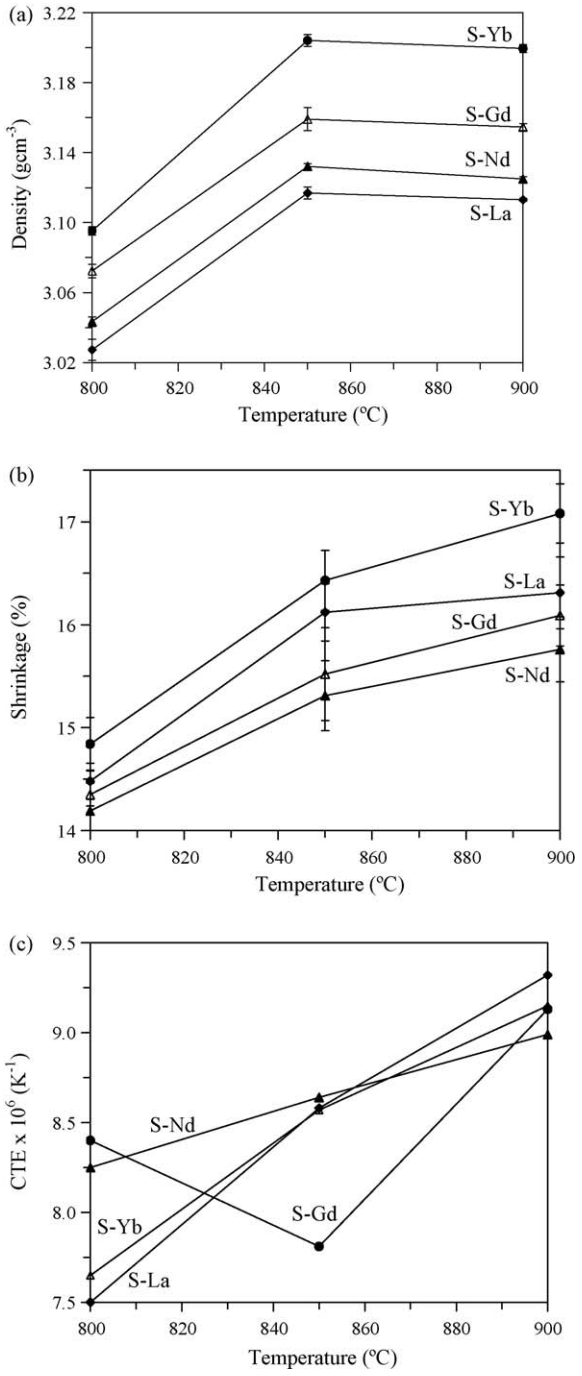


Fig. 6. Influence of temperature on: (a) density; (b) linear shrinkage; and (c) CTE of the sintered GCs.

temperature (Fig. 6c). The highest CTE at 800 °C was obtained for composition S–Gd while the lowest was obtained for S–La. With increase in temperature, S–La showed highest CTE among all the investigated GCs at 900 °C.

## 4. Conclusions

The effect of different RE-oxides on the structure, sintering ability and crystallization behaviour of diopside based GCs has been investigated. All the glasses show spinodal type of glass-in-glass phase separation. The glass containing $Nd_2O_3$ showed some peculiar properties in comparison to the glasses containing other RE-oxides. Therefore, it will be interesting to study the structure of this glass in more detail. Augite crystallized out to be the primary crystalline phase in all the GCs along with different polymorphs of celsian as secondary phases. Sintering preceded crystallization in all the four glasses. The GCs containing $Yb_2O_3$ showed highest linear shrinkage and density values in comparison to other GCs while $La_2O_3$ containing GC showed highest CTE value after heat treatment at 900 °C.

## Acknowledgements

Ishu Kansal is thankful to CICECO for research grant. The support of CICECO, University of Aveiro and FCT, Portugal (SFRH/BD/37037/2007) is kindly acknowledged.

## References

[1] W. Höland, G.N. Beall, Glass-Ceramic Technology, Am. Ceram. Soc., Westerville, Ohio, 2002.
[2] T. Nonami, S. Tsutsumi, Study of diopside ceramics for biomaterials, J. Mater. Sci. Mater. Med. 10 (1999) 475–479.
[3] I.W. Donald, B.L. Metcalfe, R.N.J. Taylor, The immobilization of high level radioactive wastes using ceramics and glasses, J. Mater. Sci. 32 (1997) 5851–6126.
[4] A. Goel, D.U. Tulyaganov, V.V. Kharton, A.A. Yaremchenko, J.M.F. Ferreira, The effect of $Cr_2O_3$ on the crystallization behaviour and properties of $La_2O_3$ containing diopside based glasses and glass-ceramics, Acta Mater. 56 (2008) 3065–3076.
[5] A. Goel, D.U. Tulyaganov, V.V. Kharton, A.A. Yaremchenko, S. Eriksson, J.M.F. Ferreira, Optimization of $La_2O_3$-containing diopside based glass-ceramic sealants for fuel cell applications, J. Power Sources 189 (2009) 1032–1043.
[6] A. Goel, D.U. Tulyaganov, E.R. Shaaban, R.N. Basu, J.M.F. Ferreira, Influence of ZnO on the crystallization kinetics and properties of Diopside-Ca-Tschermak based glasses and glass-ceramics, J. Appl. Phys. 104 (2008) 043529.
[7] S. Sen, J.F. Stebbins, Structural role of $Nd^{3+}$ and $Al^{3+}$ cations in $SiO_2$ glass: a $^{29}$Si MAS-NMR spin-lattice relaxation, $^{27}$Al NMR and EPR study, J. Non-Cryst. Solids 188 (1995) 54–62.
[8] A.I. Smirnov, S. Sen, High field electron paramagnetic resonance of $Gd^{3+}$-doped glasses: line shapes and average ion distances in silicates, J. Chem. Phys. 115 (2001) 7650.
[9] V.I. Spitsyn, G.V. Ionova, The quantum chemistry of unusual oxidation states of the lanthanides and actinides, Russ. Chem. Rev. 53 (1984) 725–743.
[10] A.B. Corradi, V. Cannillo, M. Montorsi, C. Siligardi, A.N. Cormack, Structural characterization of neodymium containing glasses by molecular dynamic simulation, J. Non-Cryst. Solids 351 (2005) 1185–1191.
[11] P. Loiseau, D. Caurant, K. Dardenne, S. Mangold, M. Denecke, J. Rothe, N. Baffier, C. Fillet, Characterisation of Nd-doped calcium aluminosilicate parent glasses designed for the preparation of zirconolite-based glass-ceramic waste forms, ATALANTE 2004: Advances for future nuclear fuel cycles, Nîmes, France, June 21–24, 2004.
[12] A.K. Varshneya, Fundamental of Inorganic Glasses, Academic Press Inc., USA, 1994, , ISBN: 0-12-714970-8.
[13] A. Quintas, D. Caurant, O. Majérus, J.-L. Dussossoy, T. Charpentier, Effect of changing rare-earth cation type on the structure and crystallization behaviour of an aluminoborosilicate glass, Phys. Chem. Glasses 49 (2008) 192–197.

[14] J.T. Kohli, R.A. Condratr, J.E. Shelby, Raman and infrared spectra of rare earth aluminosilicate glasses, Phys. Chem. Glasses 34 (1993) 81–87.
[15] L. Stoch, M. Sroda, Infrared spectroscopy in the investigation of oxide glasses structure, J. Mol. Struct. 511–512 (1999) 77–84.
[16] J.E. Shelby, J.T. Kohli, Rare-earth aluminosilicate glasses, J. Am. Ceram. Soc. 73 (1990) 39–42.
[17] F.J. Torres, J. Alarcon, Mechanism of crystallization of pyroxene based glass–ceramic glazes, J. Non-Cryst. Solids 347 (2004) 45–51.
[18] R.C. De Vekey, A.J. Majumdar, Effect of fabrication variables on the properties of cordierite based glass–ceramics. 2. Effect of composition, Glass Technol. 15 (1974) 71–80.